HYDROGEN ADSORPTION PROCESS IN NANOCRYSTALLINE NUCLEAR GRAPHITE

by

Vladimir D. LUKIĆ [1], ***Milica M. SPASOJEVIĆ*** [2*], ***Milentije D. LUKOVIĆ*** [1], ***Miroslav D. SPASOJEVIĆ*** [1], ***and Aleksa M. MARIČIĆ*** [1]

[1]Joint Laboratory for Advanced Materials of SASA, Section for Amorphous Systems, Faculty of Technical Sciences, University of Kragujevac, Čačak, Serbia
[2] Innovative Centre of the Faculty of Chemistry, University of Belgrade, Belgrade, Serbia

Scientific paper
https://doi.org/10.2298/NTRP2201011L

Kinetics and mechanism of hydrogen adsorption in as-obtained and ground nuclear graphite Wendelstein 7-X are examined. In the first time interval the adsorption process is determined by dissociation of the hydrogen molecule, occurring at the outer surface and in open micropores of nuclear graphite particles. However, in the second time interval, the slowest step in the hydrogen adsorption is inter-granular and inter-crystallite diffusion in nanopores of graphite. The X-ray analysis shows, that grinding of as-obtained nuclear graphite results in finer particles with finer nanocrystals and larger density of opened pores and carbon reactive sites. The capacity and rate of adsorption increase with comminution of nuclear graphite particles and adsorbed hydrogen does not substantially alter the microstructure of nuclear graphite.

Key words: hydrogen adsorption, porous graphite, surface area, nanocrystalline nuclear graphite, kinetic and mechanism

INTRODUCTION

Carbon materials have been of great interest for nuclear applications since they exhibit high hydrogen retention even at high temperatures [1-4]. In the next-generation advanced fission reactors, including solid fuel fluoride salt-cooled high temperature reactors [5], dissolved fuel molten salt reactors [6] and high temperature gas cooled reactors [7], carbon materials have been proposed as moderating and structural materials, where, they interact with substantial amounts of produced tritium. In fusion systems, considerable attention has been focused on determining the behavior of tritium on graphite due to their potential application as a heat-resistant, highly heat-conductive, first-wall materials [8, 9]. The worldwide use of nuclear graphite results in more than 250 000 tons of irradiated nuclear graphite that requires special treatment [10]. Tritium is rather short lived with a half-life of about 12.3 years [11]. However, after shutting down the nuclear reactor, in the first years 80-90 % activity of the irradiated nuclear graphite originates from tritium and carbon 14 [12]. Tritium could be easily released from irradiated nuclear graphite and thus, present a serious radiological health concern [13, 14]. Therefore, the removal of tritium from irradiated graphite is one of the most important aims of decontamination of nuclear graphite.

Nuclear graphite has a complex structure that differs from the ideal mono-crystallites, which are nominally composed of ABAB-stacked graphene layers. Despite chemical inertness of carbon atoms in an infinite and perfect lattice, the edges of the graphene layers and defects within them are reactive carbon sites tritium can bind for. Enthalpies of adsorption of these reactive carbon sites are different and depend on the specific chemical environment of each site. The adsorption of hydrogen (tritium) on the zig-zag and armchair edges are substantially more stable than on the perfect graphite surface [15-17], *e. g*., Lechner *et al.* [15] determined the adsorption energy, E_{ad}, for hydrogen on the perfect surface (–0.68 eV or –0.73 eV), E_{ad} for hydrogen on zig-zag and armchair edges (–4.99 eV and –3.73 eV), and E_{ad} for hydrogen on zig-zag and armchair reconstruction edges (–2.80 eV and –2.63 eV). Hydrogens are preferentially adsorbed on the adjacent carbon sites until each carbon site adsorbs the second hydrogen [4]. Armchair + 8H is considered as the most stable edge at reasonable temperature and hydrogen (or tritium) pressure [4]. Hydrogen can also firmly bind to point defects, such as mono and

* Corresponding author, e-mail: smilica84@gmail.com

di-vacancies, with less strong binding to a divacancy than to mono-vacancy [15, 18-20]. Graphite porosity is rather complex. It contains micropores among grains and nanopores, among crystallites [21]. The porosity can be either open porosity or closed porosity [21, 22]. Since hydrogen and tritium are isotopes with similar physical and chemical properties, theoretical studies with the aim of simulating the behavior of tritium in nuclear graphite are performed with hydrogen instead of tritium [14, 23, 24]. Therefore, an understanding and prediction of hydrogen behavior on carbon materials is essential for evolution of performance and safety of present and future reactor design. In general, it is considered that hydrogen chemisorbs onto graphitic material via chemical bending. However, the generally proposed mechanism has been inconsistent, *i. e*., adequate for some studies and completely improper for others [4, 8, 25, 26]. According to findings of Shirasu *et al*. [27], the adsorption isotherm followed Sievert's law, suggesting a simple dissociative adsorption process. This result is also confirmed by Strehlow [28]. Based on the results from temperature desorption studies, Atsumi *et al*. [29, 30] have proposed a co-existence of multiple adsorption and desorption modes. They suggested a hydrogen transport and adsorption model, which elucidate both porous diffusion and dissociative trapping. In this model, the edges of the graphite sheets present under-coordinated carbon atoms that have high hydrogen reactivity [29-32]. Lam *et al*. [23] found a good positive correlation between the hydrogen adsorption, and the surface area and pore volume, which is the result of the increase in available active site density. They modeled the chemisorption isotherms with several two- and three-parameter isotherms, namely the Langmuir, Temkin, Freundlich and Sips models. The kinetic and mechanism for adsorption and desorption of hydrogen in nuclear graphite and the effect of the type of graphite on these processes have been studied by many research groups [22, 29, 33-45]. Most authors considered the slow inter-granular diffusion and inter-crystallite diffusion as the slowest step of the hydrogen adsorption and desorption process. Vergari *et al*. [22] have shown that hydrogen adsorbs in nuclear graphite: (a) as H_2 in closed porosity, (b) as physiosorbed on graphitic planes, and (c) as chemisorbed at reactive carbon sites. When exposing graphite to a hydrogen gas, the H_2 molecules penetrate the sample surface, diffuse through the open pores and reach the surface grain [22]. The diffusion through the open pores is a rapid process [22]. In the closed porosity, the access of the H_2 molecules to the surface of the grains is enabled by the inter-granular and inter-crystallite diffusion. Within the graphite grain, hydrogen diffuses as a molecule via inter-crystallite diffusion (a diffusion-controlled process) and as an atom, via intra-crystallite diffusion (a reaction-kinetics-controlled process) [22]. The inter-crystallite diffusion process is decelerated by adsorption at reactive carbon sites. The intra-crystallite diffusion starts with dissociation of hydrogen atoms. The dissociated atoms diffuse between graphite-based planes and are finally adsorbed at the reactive carbon site [22]. The reaction-kinetics-controlled process is attributed to molecular dissociation. Hydrogen desorption has a different rate-limiting step and kinetics that depend on the way the hydrogen is kept in the graphite: molecular hydrogen confined in closed pores desorbs through a diffusion-controlled process [22], hydrogen dissolved as a solid solution on graphite basal plane is desorbed through a recombination-controlled process [22], hydrogen adsorbed at edges desorbs through an inter-crystallite diffusion-controlled [43] or, a recombination-controlled process [44], and hydrogen adsorbed in vacancies desorbs through a desorbing-controlled process [43]. However, in spite of a large number of publications regarding this subject, kinetics and mechanism of hydrogen adsorption and desorption has not been clarified yet. Thus, the aim of this study was to investigate the effect of the relative density of open pores on the kinetics and mechanism of hydrogen adsorption in nuclear graphite. Also, it was examined how the adsorption process affected the microstructure of graphite.

EXPERIMENTAL

In order to investigate kinetics of the hydrogen adsorption, as-obtained and ground samples of nuclear graphite Wendelstein 7-X were used. Graphite was ground in a planetary ball mill (Retsch PM-400). The grinding time of the powder was from 50 to 130 min. Hydrogen adsorption and an effect of adsorption on microstructure of as-obtained and ground powders were examined. Adsorption of hydrogen is performed using a chamber, with the thermoregulation system and different mercury pressure gauge. The volume of the chamber was 120.53 cm^3. Samples were de-gassed prior to hydrogenation. The hydrogen adsorption was measured: (a) during the sample heating from 30 to 160 °C, by rate 14 °Cmin^{-1} and (b) under isothermal conditions at temperature of 70 °C.

The X-ray diffraction patterns of samples were obtained using a Bruker DM (XRD) instrument in Bragg-Brentano geometry with a grazing incidence angle of 0.5° using CuK (λ_k = 0.154 nm) radiation. Diffraction data were acquired over the scattering angle 2θ from 10° to 90° with step of 0.05°.

RESULTS AND DISCUSSION

The hydrogen adsorption on nuclear powders, ground for 50, 90, and 130 minutes, is studied. During the adsorption process, pressure inside the chamber with the graphite sample, is determined. Dependance of pressure on the time of hydrogen adsorption, on the samples of nuclear graphite, is shown in fig. 1.

Figure 1 shows that initial time interval is characterized by the exponential pressure drop. In the following (second) time interval the pressure drop is slower,

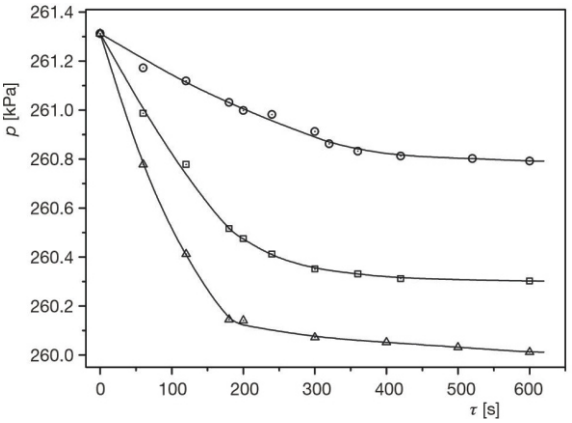

Figure 1. Hydrogen pressure as a function of adsorption time on the samples of nuclear graphite ground for: ○ – 50 minutes, □ – 90 minutes, and △ – 130 minutes. Temperature inside the chamber was 70 °C

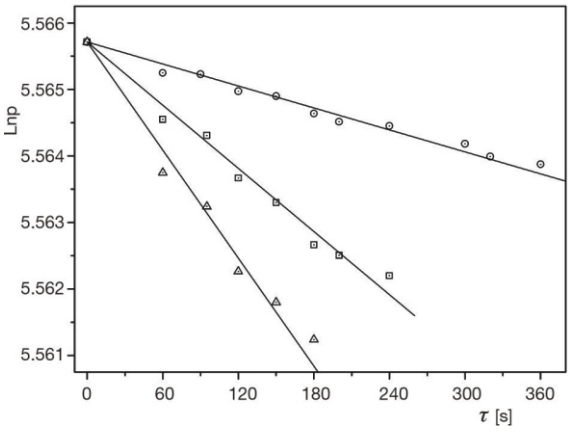

Figure 2. Logarithm of the hydrogen pressure Ln*p* as a function of time τ on nuclear graphite ground for: ○ – 50 minutes, □ – 90 minute, and △ – 130 minute at temperature of 70 °C

whereas after a longer period of time the pressure asymptotically approaches to the final value. The samples of examined nuclear graphite are porous and contain open micropores. The diffusion process in these micropores is rapid and thus, during the adsorption process the hydrogen pressure inside pores is equalized with that in the chamber. At the outer surface of graphite particles and the graphite surface in pores, the hydrogen molecules and surface carbon atoms collide. During collision between hydrogen molecules, whose energy is greater than the energy of activation of dissociation of H_2 molecules, the following reaction occurs

$$H_2 \quad C_2 \quad 2CH \tag{1}$$

The adsorbed hydrogen atoms, formed in this reaction, reach reactive carbon sites by rapid surface diffusion, where they are chemisorbed.

The rate of reaction (1) is determined from the following eq

$$\frac{dc(H_2)}{d\tau} \quad k_2 c(H_2)N(C_t) \tag{2}$$

where $c(H_2)$ – concentration of hydrogen in the chamber, τ-time, k_2 – rate constant and $N(C_t)$ – the total number of carbon atoms at the outer surface of graphite particles and the graphite surface in open micropores. At the outer surface and the surface of open pores, reactive carbon sites are zig-zag and armchair, and reconstructed zig-zag and armchair edges. Adsorption of hydrogen at reactive carbon sites reduces the total number of available free C atoms at the graphite surface. However, this effect is negligible since the number of reactive carbon sites $N(C_R)$ is substantially lower than the total number of surface C atoms, $N(C_t)$. Therefore

$$N(C_t) \quad \text{const} \tag{3}$$

and

$$\frac{dc(H_2)}{d\tau} \quad kc(H_2) \tag{4}$$

$$k \quad k_2 N(C_t) \tag{5}$$

Separation of variables in the eq. (4) and integration with boundaries from $c_0(H_2)$ to $c(H_2)$ and from $\tau = 0$ to $\tau = \tau$ result in

$$c(H_2) \quad kc_0(H_2)\exp(\ k\ \tau) \tag{6}$$

From the eq. (6) a linear dependance of $\ln c(H_2)$ on τ is obtained. Since

$$c \quad \frac{p}{RT} \tag{7}$$

then there is a linear dependence of logarithm of the hydrogen pressure in the chamber, on time of adsorption occurrence. Where R – is the universal gas constant and T – temperature expressed in Kelvin. Figure 2 shows the dependance of lnp on τ in the initial (first) time interval of the hydrogen adsorption process.

Diagram from fig. 2 shows that the experimental results corroborate the theoretically obtained dependance, described by the eq. (6). These findings indicate that in the initial time interval, the hydrogen adsorption on nuclear graphite, is a pseudo first-order reaction, with dissociation of hydrogen molecules as the rate determining step. With increasing the grinding time a slope of line lnp-τ raises, whereas the length of initial time interval declines, fig. 2. The increase in grinding time results in finer graphite particles and thus, the larger total outer surface area and a greater number of surface carbon atoms per unit weight of the sample. According to eq. (5), this effect causes the increase in both the value of constant k and the slope of lines ln-τ. From the eq. (5), it was determined that the increase in grinding time from 50-90 minutes and finally 130 minutes, results in the increase of the number reactive carbon sites with $N^{50}(C_t)$ at 3.4 $N^{50}(C_t)$ and 5.5 $N^{50}(C_t)$. A particle comminution of nuclear graphite causes a quicker increase in the number of surface carbon atoms than the number of reactive carbon sites, resulting in decline in the length of the initial time interval of the hydrogen adsorption. In the second time interval, the rate determin-

ing step in the hydrogen adsorption process on nuclear graphite is the inter-granular diffusion of molecular hydrogen in nanopores to closed pores and carbon reaction sites (zig-zag, armchair and, reconstructed zig-zag and armchair edges) and inter crystallite diffusion of molecular hydrogen in nanopores to carbon reactive sites. The intra-crystallite diffusion of atomic hydrogen between graphite basal planes to mono-vacancies and di-vacancies occurs simultaneously. In nuclear graphite, the intra-crystallite diffusion is substantially less evident than simultaneous inter crystallite diffusion. In the second time interval, the rate-determining step is non-stationary diffusion of hydrogen in nanopores. As a result of this diffusion, the coverage degree of carbon active sites in nanopores with hydrogen increases. Greater coverage decelerates the rate of non-stationary diffusion, $dp/d\tau$. Solution of the equation for non-stationary diffusion indicates the linear dependance between the rate of diffusion expressed as $dp/d\tau$ and $\tau^{-0,5}$. The data from fig. 1 was used to determine values for the rate of diffusion $dp/d\tau$ and $\tau^{-0,5}$ in the second time interval. Dependance of $dp/d\tau$ on $\tau^{-0,5}$ is shown in fig. 3.

The obtained linear dependance between $dp/d\tau$ and $\tau^{-0,5}$, shown in fig. 3, corroborates that the rate of the hydrogen adsorption process in the second-time interval is determined by the slow diffusion.

The hydrogen adsorption on nuclear graphite is observed during the sample heating from 30 °C to 160 °C with a heating rate of 14 °C min^{-1}. Figure 4 shows dependance of pressure on temperature in the absence, p_e and the presence of graphite sample, p_p. The pressure difference, $p = p_e - p_p$, as a function of temperature is also presented in this figure.

As shown in fig. 4, the adsorption starts at around 60 °C. Below this temperature, energy of the hydrogen molecule is insufficient to overcome the activation energy of the dissociation reaction (reaction 1). In the temperature range of 60 to 105 °C adsorption exponentially increases. In this temperature interval, the sample is heated to 105 °C for 192 seconds. As

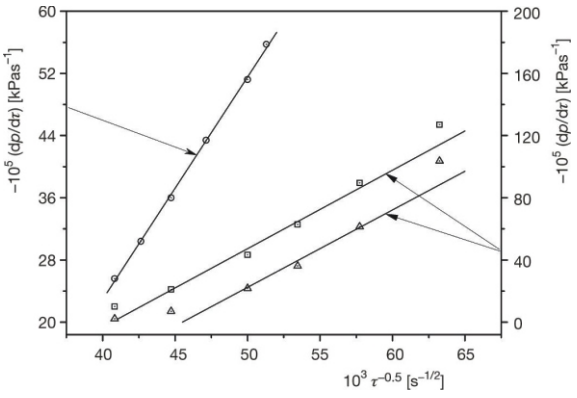

Figure 3. The rate of hydrogen diffusion, $dp/d\tau$, in ground nuclear graphite as a function $\tau^{-0,5}$ at 70 °C. Graphite is ground for: ○ – 50 minutes, □ – 90 minutes and △ – 130 minutes

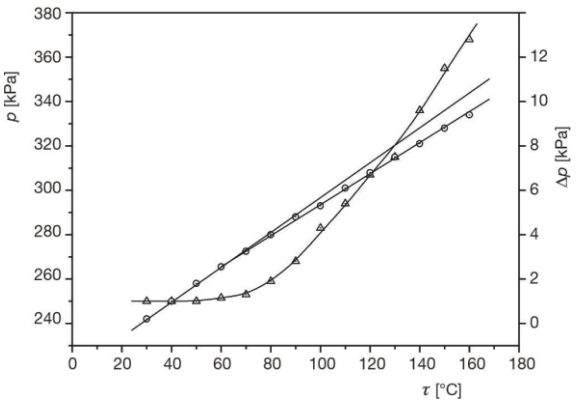

Figure 4. The pressure in the chamber as a function of temperature in: – the absence, ○ – presence of graphite sample, and – the pressure difference, p, as a function of temperature. The heating rate of the sample ground for 130 minutes is 14 °C min^{-1}

shown in fig. 2, the rate of the adsorption process in this time interval and at these temperatures is determined by dissociation of hydrogen molecules (reaction 1). This chemical reaction, according to the Arrhenius equation, exponentially rises with increasing temperature. In the temperature range of 105 °C to 160 °C, the increase in temperature and adsorption time results in linear increase in the adsorption rate, fig. 2. In this temperature and time interval, in accordance with fig. 2, the adsorption rate is determined by slow inter-granular and inter-crystallite diffusion of molecular hydrogen to carbon reactive sites in nanopores. Under these circumstances, non-stationary diffusion in nanopores is a complicated function of time and temperature [22-24, 29-45].

Adittionaly, with increasing temperature the intensity of intra-crystallite diffusion of atomic hydrogen between graphite basal planes to mono-vacancies, di-vacancies and other carbon reactive sites also increases. The diffusion rate is as well affected by the shape of function of nanopores size distribution [4]. Properties of this function depend on a degree of irradiation of nuclear graphite and grinding time, as demonstrated in this study [21-24, 29-47]. Nuclear graphite exposed to irradiation changes its microstructure with time. Crystallinity declines and thus the number of reactive carbon sites increases. In order to examine the effect of the particles and nanocrystals size as well as density of reactive carbon sites, nuclear graphite is ground for different periods of time in a planetary ball mill. Subsequently, the microstructure of the ground powders is determined. The effect of microstructure on the hydrogen adsorption is analyzed. The XRD analysis is used to determine microstructural properties of as-obtained nuclear graphite. The XRD pattern exhibits a relatively sharp diffraction peak at about 26.4°, which corresponds to the reflection in the (002) plan of graphite layers, and four less pronounced peaks at about 42.5°, 43.7°, 54.2° and 77.8° for graphite planes (100), (101), (004), and (110), fig. 5.

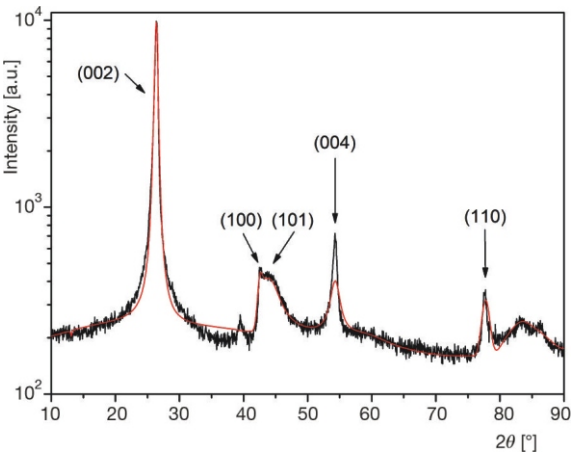

Figure 5. The XRD pattern of the as-obtained nuclear graphite

The XRD pattern of graphite shows two characteristic peaks. The (002) peak originates from the orientation of the aromatic ring carbon reticulated layer in three-dimensional arrangement. The second characteristic peak is the (100) peak, which is attributed to the degree of condensation of the aromatic ring, referring to the size of the carbon mesh slice of the aromatic ring. The narrower and the higher the (100) peak, the larger the size of the aromatic layer slice [35]. The afore-mentioned theory and the XRD-results indicate the existence of very small graphite microcrystalline structures in nuclear graphite. Grinding of nuclear graphite causes a decrease in the intensities of the all diffraction peaks and widening of their half heights, compared to as-obtained nuclear graphites. This finding indicates the decrease in stacking structure of the aromatic layer in the ground nuclear graphite, fig. 6. Therefore, grinding of nuclear graphite results in finer particles that consist of finer nanocrystals with higher density of carbon reactive sites and greater density of open pores.

In order to examine an effect of hydrogenation on microstructure, diffractograms of a hydrogenated

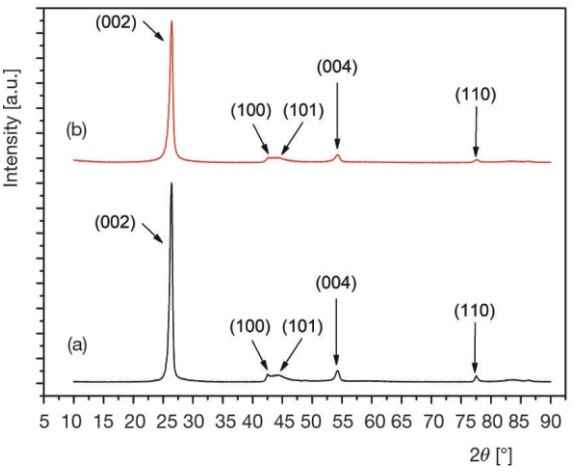

Figure 6. The XRD patterns: (a) as-obtained nuclear graphite and (b) nuclear graphite ground for 50 minutes

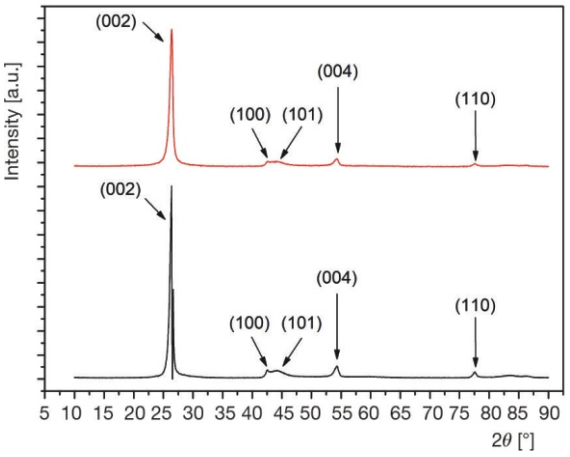

Figure 7. The XRD patterns of hydrogenated samples of: (a) as-obtained nuclear graphite and (b) nuclear graphite ground for 30 minutes

sample of as-obtained nuclear graphite, and hydrogenated and ground sample of nuclear graphite are recorded, fig. 7.

Diffraction peaks of both hydrogenated samples, fig. 7 are of same intensity and have the identical widths at half heights, as the diffraction peaks of non-hydrogenated samples, fig. 6. This indicates that the sample hydrogenation does not cause collision of nanocrystals in nuclear graphite. However, the 2θ peaks maximums of the plane (002) of the hydrogenated powders is slightly shifted towards lower angles. The shift is marginally greater for powders ground for longer times. This finding suggests that the graphite nanocrystalline layers spacing (d002) is getting higher for the hydrogenated samples [34]. The XRD analysis reveals a higher adsorption capacity of nuclear graphite with finer particles composed of finer nanocrystals, and also corroborates hydrogen chemisorption manly on zig-zag and armchair edges, and the zig-zag and armchair reconstruction edges. The increase in point defects, mono and di-vacancies, during grinding is of substantially lower intensity than the increase of carbon reaction sites located at the edges of graphite layers.

CONCLUSION

In this paper, the kinetics and mechanism of hydrogen adsorption on as-obtained and ground samples of nuclear graphite Weldenstein 7-X were determined. The samples were ground for 50, 90, and 130 minutes. For all the samples, in the initial time interval, the adsorption rate was determined by the pseudo first-order reaction, *i. e*., dissociation of the hydrogen molecules, which occurred at the outer surface and in open micropores of nuclear graphite particles. In the second time interval, the rate determining step in the mechanism of the adsorption process, was inter-granular and inter-crystalline diffusion of molecular hydrogen in nanopores, to carbon reactive sites. The X-ray analysis

revealed that the as-obtained and ground samples were composed of nanocrystals. With increasing grinding time, finer particles with lower mean size of nanocrystals, larger density of open nanopores and greater number of carbon reactive sites were formed. The nuclear graphite, with larger number of carbon reactive sites showed the higher capacity for the hydrogen storage and faster occurrence of adsorption on this sample. Adsorbed hydrogen did not deteriorate the crystalline lattice of nuclear graphite. The sample hydration just slightly increased the graphite nanocrystalline layer spacing, d002.

AKNOWLEDGMENT

This work was funded by the Ministry of Education, Science and Technological Development of the Republic of Serbia [Project Ref. No. 170257 and Grant No. 451-03-68/2022-14/200288, Innovative Centre of the Faculty of Chemistry, University of Belgrade].

AUTHORS' CONTRIBUTIONS

M. D. Spasojević and A. M. Maričić concepted the research, processed and analyzed the obtained results and finalized the article writing. M. M. Spasojević analyzed the obtained results and finalized the article writing. V. D. Lukić and M. D. Luković performed the experimental work, processed results, and wrote the original draft.

REFERENCES

[1] Atsumi, H., *et al.*, Hydrogen Solubility and Diffusivity in Neutron-Irradiated Graphite, *J. Nucl. Mater., 191-194* (1992), Part A, pp. 368-372
[2] Atsumi, H., *et al.*, Trapping and Detrapping of Hydrogen in Carbon-Based Materials Exposed to Hydrogen Gas, *J. Nucl. Mater., 212-215* (1994), Part B, pp. 1478-1482
[3] Li, J., *et al.*, Recent Advances in the Treatment of Irradiated Graphite: A Review, *Ann. Nucl. Energy, 110* (2017), Dec., pp. 140-147
[4] Zhang, M., *et al.*, Tritium Adsorption and Desorption on/from Nuclear Graphite Edge by a First-Principles Study, *Carbon N. Y., 173* (2021), Mar., pp. 676-686
[5] Forsberg, C., Peterson, P. F., Basis for fluoride Salt-Cooled High-Temperature Reactors with Nuclear Air-Brayton Combined Cycles and Firebrick Resistance-Heated Energy Storage, *Nucl. Technol., 196* (2016), 1, pp. 13-33
[6] Thoma, R. E., Chemical Aspects of MSRE Operation, ORNL-4658, Oak Ridge National Laboratory, Oak Ridge, Tennessee, 1971
[7] Rohrig, H. D., *et al.*, Tritium Balance in High Temperature Gas Cooled Reactors, *J. Am. Ceram. Soc., 59* (1976), 7-8, pp. 316-320
[8] Causey, R. A., *et al.*, Tritium Barriers and Tritium Diffusion in Fusion Reactors, *Comprehensive Nuclear Materials, 4* (2012), pp. 511-549
[9] Andrew, P., Pick, M., Hydrogen Retention in the first Wall, *J. Nucl. Mater., 220-222* (1995), Apr., pp. 601-605
[10] Telling, R. H., Heggie, M. I., Radiation Defects in Graphite, *Philos. Mag., 87* (2007), 31, pp. 4749-4846
[11] Lucas, L. L., Unterweger, M. P., Comprehensive Review and Critical Evaluation of the Half-Life of Tritium, *J. Res. Natl. Inst. Stand. Technol., 105* (2000), 4, pp. 541-549
[12] Buchuev, A. V., *et al.*, Quantitative Determination of the Amount of ^{3}H and ^{14}C in Reactor Graphite, *At. Energy, 73* (1992), 6, pp. 959-962
[13] Zhengkun, T., *et al.*, Radiation Protection on Tritium Internal Exposure at Third Qinshan Nuclear Power Plant, *Radiat. Prot. Bull., 27* (2007), 4, pp. 34-38
[14] Li, H., *et al.*, Experimental Study on the Adsorption and Desorption of Tritium in the Graphite Materials for HTR-PM, *Prog. Nucl. Energy, 85* (2015), Nov., pp. 676-681
[15] Lechner, C., *et al.*, Adsorption of Atomic Hydrogen on Defect Sites of Graphite: Influence of Surface Reconstruction and Irradiation Damage, *Carbon N. Y., 127* (2018), pp. 437-448
[16] Nguyen, H. T., *et al.*, Migration and Desorption of Hydrogen Atom and Molecule on/from Graphene, *Carbon N. Y., 121* (2017), Sept., pp. 248-256
[17] Yang, F. H., Yang, R. T., Ab Initio Molecular Orbital Study of Adsorption of Atomic Hydrogen on Graphite: Insight Into Hydrogen Storage in Carbon Nanotubes, *Carbon N. Y., 40* (2002), 3, pp. 437-444
[18] Wu, X. J., *et al.*, Adsorption and Desorption of Hydrogen on/from Single-Vacancy and Double-Vacancy Graphenes, *Nucl. Sci. Tech., 30* (2019), 4, pp. 1-9
[19] Casartelli, M., *et al.*, Structure and Stability of Hydrogenated Carbon Atom Vacancies in Graphene, *Carbon N. Y., 77* (2014), Oct., pp. 165-174
[20] Sunnardianto, G. K., *et al.*, Storing-Hydrogen Processes on Graphene Activated by Atomic-Vacancies, *Int. J. Hydrogen Energy, 42* (2017), 37, pp. 23691-2369
[21] Mays, T. J., A New Classification of Pore Sizes, *Stud. Surf. Sci. Catal., 160* (2007), pp. 57-62
[22] Vergari, L., Scarlat, R. O., Kinetics and Transport of Hydrogen in Graphite at High Temperature and the Effects of Oxidation, Irradiation and Isotopics, *J. Nucl. Mater., 558* (2022), pp. 1-19
[23] Lam, S. T., *et al.*, Modeling and Predicting Total Hydrogen Adsorption in Nanoporous Carbon Materials for Advanced Nuclear Systems, *J. Nucl. Mater., 511* (2018), Dec., pp. 328-340
[24] Deng, K., *et al.*, Adsorption and Desorption of Tritium in Nuclear Graphite at 700 °C: A Gas Chromatographic Study Using Hydrogen, *Nucl. Technol., 205* (2019), 9, pp. 1143-1153
[25] Redmond, J. P., Walker, P. L., Hydrogen Sorption on Graphite at Elevated Temperatures, *J. Phys. Chem., 64* (1960), 9, pp. 1093-1099
[26] Causey, R. A., The Interaction of Tritium with Graphite and Its Impact on Tokamak Operations, *J. Nucl. Mater., 162-164* (1989), Part C, pp. 151-161
[27] Shirasu, Y., *et al.*, Solubility of Hydrogen Isotopes in Graphite, *J. Nucl. Mater., 179-181* (1991), 1, pp. 223-226
[28] Strehlow, R. A., Chemisorption of Tritium on Graphites at Elevated Temperatures, *J. Vac. Sci. Technol. A Vacuum, Surfaces, Film., 4* (1986), 3, pp. 1183-1185

[29] Atsumi, H., Hydrogen Retention in Graphite and Carbon Materials Under a Fusion Reactor Environment, *J. Nucl. Mater., 313-316* (2003), Mar., pp. 543-547
[30] Atsumi, H., *et al.*, Trapping State of Hydrogen Isotopes in Carbon and Graphite Investigated by Thermal Desorption Spectrometry, *Fusion Sci. Technol., 67* (2015), 2, pp. 245-249
[31] Arboleda, N. B., *et al.*, Scattering and Dissociative Adsorption of H2 on the Armchair and Zigzag Edges of Graphite, *J. Appl. Phys., 96* (2004), 11, pp. 6331-6336
[32] Dino, W. A., *et al.*, H2 Dissociative Adsorption at the Armchair Edges of Graphite, *Solid State Commun., 132* (2004), 10, pp. 713-718
[33] Atsumi, H., Mechanism of Hydrogen Trapping and Transport in Carbon Materials, *Phys. Scr., 2003* (2003), T103, pp. 77-80
[34] Li, W., Zhu, Y., Structural Characteristics of Coal Vitrinite During Pyrolysis, *Energy and Fuels, 28* (2014), 6, pp. 3645-3654
[35] Malka, V., *et al.*, Investigations on Sorption and Diffusion of Tritium in HTGR-Graphite, *Int. J. Appl. Radiat. Isot., 31* (1980), 8, 469
[36] Atsumi, H., Kondo, Y., Retention and Release of Hydrogen Isotopes in Carbon Materials Priorly Charged in Gas Phase, *Fusion Eng. Des., 131* (2018), June, pp. 49-53
[37] Atsumi, H., *et al.*, Hydrogen Behavior in Carbon and Graphite Before and After Neutron Irradiation – Trapping, Diffusion and the Simulation of Bulk Retention, *J. Nucl. Mater., 417* (2011), 1, pp. 633-636
[38] Robell, A. J., *et al.*, Surface Diffusion of Hydrogen on Carbon, *J. Phys. Chem., 68* (1964), 10, pp. 2748-2753
[39] Tsuchiya, B., Morita, K., Retention of H and D in Graphite by Simultaneous H+ and D+ Ion Implantation, *J. Nucl. Mater., 227* (1996), 3, pp. 195-202
[40] Atsumi, H., Tauchi, K., Hydrogen Absorption and Transport in Graphite Materials, *J. Alloys Compd, 356-357* (2003), Aug., pp. 705-709
[41] Atsumi, H., *et al.*, Bulk Hydrogen Retention in Neutron-Irradiated Graphite at Elevated Temperatures, *J. Nucl. Mater., 390-391* (2009), 1, pp. 581-584
[42] Atsumi, H., Iseki, M., Hydrogen Absorption Process Into Graphite and Carbon Materials, *J. Nucl. Mater., 283-287* (2000), Part II, pp. 1053-1056
[43] Atsumi, H., *et al.*, Thermal Desorption of Hydrogen from Carbon and Graphite at Elevated Temperatures, *J. Nucl. Mater., 438* (2013), Suppl. pp. S963-S966
[44] Hoinkis, E., The Chemisorption of Hydrogen on Porous Graphites at Low Pressure and at Elevated Temperature, *J. Nucl. Mater., 182* (1991), Part C, pp. 93-106
[45] Kanashenko, S. L., Hydrogen Adsorption on and Solubility in Graphites, *J. Nucl. Mater., 233-237* (1996), Part 2, pp. 1207-1212
[46] Ćirović, N., *et al.*, Synthesis, Structure and Properties of Nickel-Iron-Tungsten Alloy Electrodepoisits PART II: Effect of Microstructure on Hardness, Electrical and Magnetic Properties, *Sci. Sinter., 48* (2016), 1, pp. 1-16
[47] Ćirović, N., *et al.*, Synthesis, Structure and Properties of Nickel-Iron-Tungsten Alloy Electrodepoisits PART I: Effect of Sythesis Parameters on Chemical Composition, Microstructure and Morphology, *Sci. Sinter., 47* (2015), 3, pp. 347-365

Received on May 26, 2022
Accepted on June 14, 2022

Владимир Д. ЛУКИЋ, Милица М. СПАСОЈЕВИЋ, Милентије Д. ЛУКОВИЋ, Мирослав Д. СПАСОЈЕВИЋ, Алекса М. МАРИЧИЋ

АДСОРПЦИЈА ВОДОНИКА У НАНОКРИСТАЛНОМ НУКЛЕАРНОМ ГРАФИТУ

Детерминисана је кинетика и механизам адсорпције водоника у свежем и млевеном нуклеарном графиту Wendelstein 7-X. Показано је да у првом временском интервалу брзину процеса адсорпције одређује дисоцијација молекула водоника која се одвија на спољној површини и у отвореним микропорама нуклеарног графита. У другом временском интервалу најспорији ступањ у процесу адсорпције водоника је дифузија у нанопорама лоцираним између честица и између кристала нуклеарног графита. Анализом помоћу X-зрака установљено је да млевењем свежег нуклеарног графита настају ситније честице са ситнијим нанокристалима и већом густином отворених пора и реактивних атома угљеника. Капацитет и брзина адсорпције расту са уситњавањем честица нуклеарног графита. Адсорбовани водоник значајније не мења микроструктуру нуклеарног графита.

Кључне речи: адсорпција водоника, порозан графит, површина, нанокристални нуклеарни графит, кинетика и механизам